CABRI EXPERIMENTAL REACTOR: EXPERIMENTAL REASSESSMENT OF CABRI CORE POWER AND MEASUREMENT UNCERTAINTIES

F. JEURY*, L. PANTERA, Y. GARNIER
CEA[1], DEN[2], Cadarache research centre, Reactor Studies Department, 13108 Saint-Paul-Lez-Durance, France

*Corresponding author: florence.jeury@cea.fr

ABSTRACT

The CABRI experimental reactor operated by CEA is located at the Cadarache research centre, in southern France. The common objective of the programmes that have been conducted on CABRI since 1978 is the study of fuel rod behaviour under Reactivity Initiated Accident (RIA) conditions.

The CABRI experimental reactor includes an experimental loop specially designed to position in the centre of the driver core the instrumented test device housing the fuel pin to be tested, and to cool the tested fuel rod into the required thermohydraulic conditions.
Initially designed for safety studies on FBR's fuels the experimental loop was a sodium loop. In view of the burn-up increase of PWR's fuels (optimization of PWR core management) the facility was modified in order to have a water loop able to provide thermohydraulic conditions representative of the nominal operating PWR's ones (155 bar, 300°C).

This programme which began in 2003 lied within a broader scope including an overall facility refurbishment and a safety review.

In this framework, an experimental method was defined to assess the power of the CABRI core, and thus, the injected energy in the experimental fuel rod. In particular, this method will take into account the ingress of pool water into the newly designed upper water box during thermal balances performed on the core water cooling circuit (calibration phase of the neutron power chambers). Uncertainties of about 4 % and 11 % are expected respectively on the core power measurement and on the injected energy in the tested fuel rod.

1 Introduction

The CABRI experimental reactor operated by CEA is located at the Cadarache research center, in southern France. The common objective of the programmes that have been performed on CABRI since 1978 is the study of the fuel rod behaviour under Reactivity Initiated Accident (RIA) conditions.

The CABRI experimental reactor includes an experimental loop specially designed to position in the centre of the driver core the instrumented test device housing the fuel rod to be tested, and to cool this fuel rod into the required thermohydraulic conditions.

Initially designed for safety studies on FBR's fuels the experimental loop was a sodium loop. In view of the burn-up increase of PWR's fuels (optimization of PWR core management) the facility was modified in order to have a water loop able to provide thermohydraulic conditions representative of the nominal operating PWR's ones (155 bar, 300°C).

This project which began in 2003 lied within a broader scope including an overall facility refurbishment and a safety review. The global modification is conducted by the CEA project team. It is financed by IRSN[3] in the framework of an international collaboration.

In this framework, an experimental method was defined to assess the power of the CABRI core, and thus, the injected energy in the experimental fuel rod.

After a description of the facility and of the different programmes conducted on CABRI, this paper will explain why a new experimental method had to be defined to assess the driver

[1] CEA : Commissariat à l'Energie Atomique et aux Energies Alternatives.
[2] DEN : Direction de l'Energie Nucléaire.
[3] IRSN : Institut de Radioprotection et de Sûreté Nucléaire.

core power, and thus, to assess the injected energy in the experimental fuel rod. Then, it will describe the experimental methodology itself, including the assessment of measurement uncertainties.

2 The CABRI facility

The CABRI experimental reactor (see Fig.1) is an open pool-type research reactor composed of a driver core, 80 cm high, 60 cm length, 60 cm wide, made of 1488 UO_2 rods enriched with 6 % of ^{235}U. These rods have been specially designed to support an injection of reactivity (austenitic steel cladding, large pellet/cladding gap). In steady-state conditions the core power is controlled through 6 Hafnium control rods up to a maximum power of 25 MW. The core is cooled by a forced water flow of 3200 m^3/h when the core power is upper 100 kW, and by natural convection with the pool water when the core power is lower.

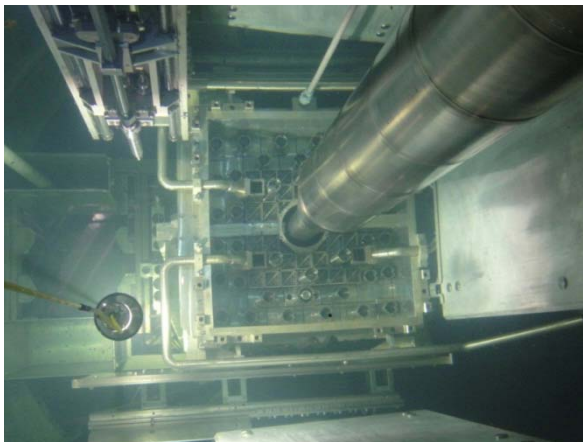

Fig.1: Reloaded CABRI core (April 2013)

CABRI includes also an experimental loop specially designed to (see Fig. 2):

- receive in the centre of the driver core the instrumented test device housing the fuel rod to be tested; this device includes also the instrumentation to control the experiment and to characterise the behaviour of the fuel rod during the power burst,
- cool the experimental fuel rod into the required thermohydraulic conditions.

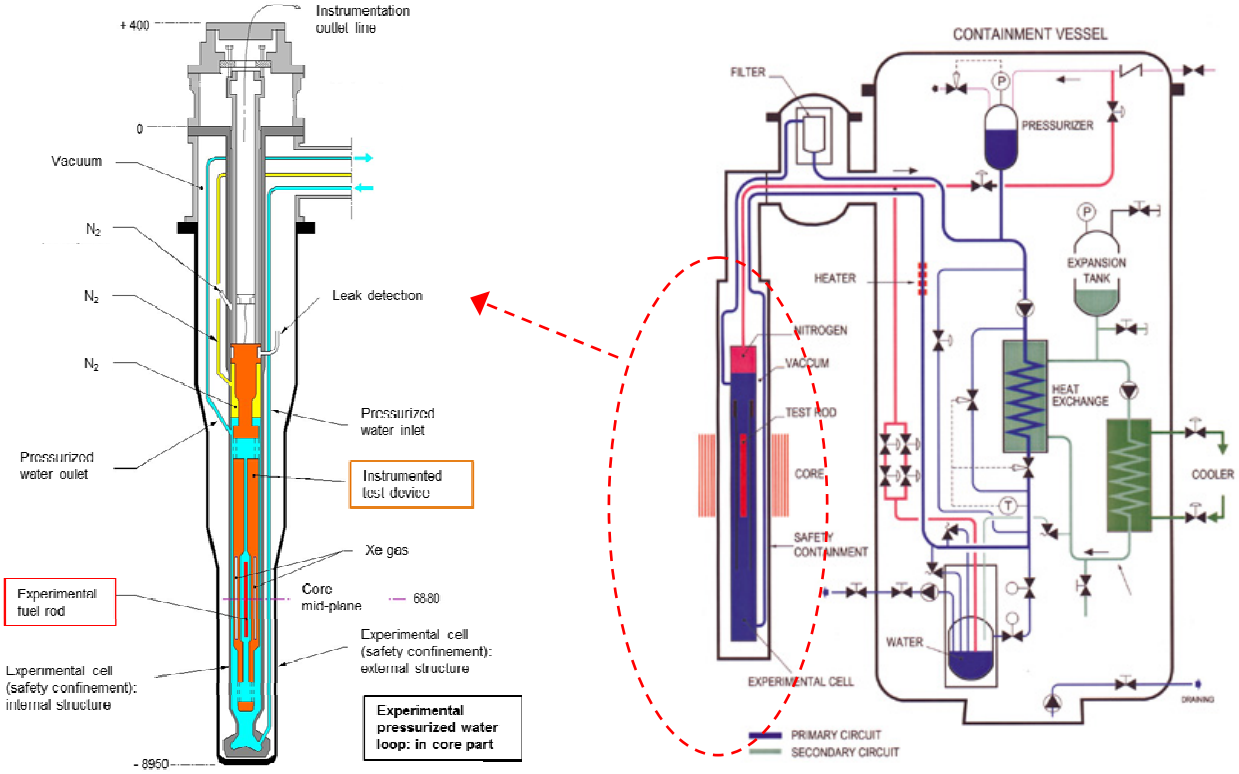

Fig. 2. Experimental pressurized water loop: 155 bar, 300°C

One of the main features of CABRI reactor is its reactivity injection system: four driver core assemblies are fitted with cylindrical tubes at their periphery. These tubes, called “transient rods”, can be pressurised with ^{3}He gas (neutron absorber) up to 15 bars then depressurised extremely quickly into a vacuum tank by opening fast valves. This causes a reactivity injection. Thus, the core power bursts up to 20 GW for example (see Fig. 3) in a few ten of ms before dropping just as quickly owing to neutron feedbacks (mostly Doppler effect). This power excursion can lead to the failure of the experimental rod clad as well as to the possible ejection of a part of its fuel into the experimental loop coolant.

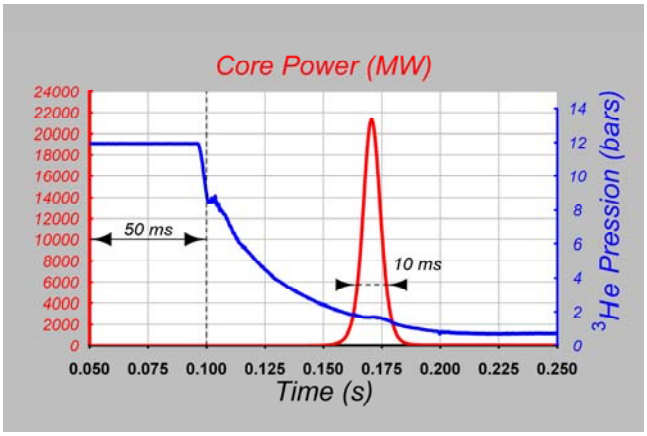

Fig. 3. Core power transient and ^{3}He pressure (exemple of measurements)

3 The CABRI programmes

The CABRI facility was originally devoted to the study of fast breeder reactors (FBR) fuel pin behaviour submitted to a power transient simulating sodium vaporization in the core and an ejection of a control rod. Thus, the experimental loop was a sodium cooling one. Between 1978 and 2001, 59 experiments were performed on Superphenix and Phenix fuel pin types in the framework of 4 international programmes: CABRI 1, CABRI 2, CABRI FAST, and CABRI RAFT programmes.

In view of the burn-up increase of PWR’s fuels (optimization of PWR core management), a first programme was already carried out in the sodium cooling experimental loop : the REPNa programme. This programme was devoted to study the behaviour of both UO_2 and MOX highly irradiated fuels submitted to fast power transients simulating RIA, and to identify the main phenomena which can lead to rod failure and possible fuel ejection. From 1993 to 2000, twelve tests were conducted, eight on UO_2 fuels, and four on MOX fuels, with a burn-up reaching up to 65 GWd/tM.

New tests are now necessary to study the behaviour of even more irradiated UO_2 and MOX fuels (up to 100 GWd/tM) in thermohydraulic conditions representative of PWR ones and to estimate the safety criteria margins on present and new fuel types (thresholds for cladding failure and fuel dispersion).
In this framework, in 2001, IRSN, in partnership with EDF[4] and with a broad international cooperation, initiated a new research programme in the CABRI facility under OECD auspices: the CABRI International Programme (CIP).

The first two CIP tests were performed on November 2002 in the sodium cooling loop. They consisted in submitting two highly irradiated PWR UO_2 fuels (burn-up around 75 GWd/tM) with advanced claddings to typical RIA power excursions.

The other CIP tests will be carried out in the new experimental water loop that replace the sodium loop, able to provide thermohydraulic conditions representative of the nominal operating PWR’s ones (155 bar, 300°C).

The facility modification conducted by the CEA project team lasted 7 years, from 2003 to

[4] EDF: Electricité De France.

2010. It included the sodium loop dismantling, the implementation of the new pressurized water loop, and an overall facility refurbishment and a safety review [1]. A commissioning tests phase is now under way [2], [3], [4], [5].

4 Reassessment of the CABRI core power

4.1 Context

During the seismic reinforcement of the facility, works were undertaken going from significant civil works to modification of several systems.

Thus, to prevent damages on the Hafnium control rods in case of an earthquake, the passage of these control rods through the upper box was expanded.

Computations were performed with the 3D TRIO-U code developed by CEA. They highlighted a mixing zone (see Fig. 4) in the newly designed upper water box area during the reactor forced cooling phase: ingress of pool water into the upper water box and, at the same flow (q) as the pool level remains constant, outlet of the reactor coolant into the pool (see Fig. 4 and Fig. 5). This calculated flow reaches ~11 % of the reactor cooling flow rate which corresponds to a calculated thermal leak of 2.3 MW for a temperature difference of 10°C between the core coolant and the pool water.

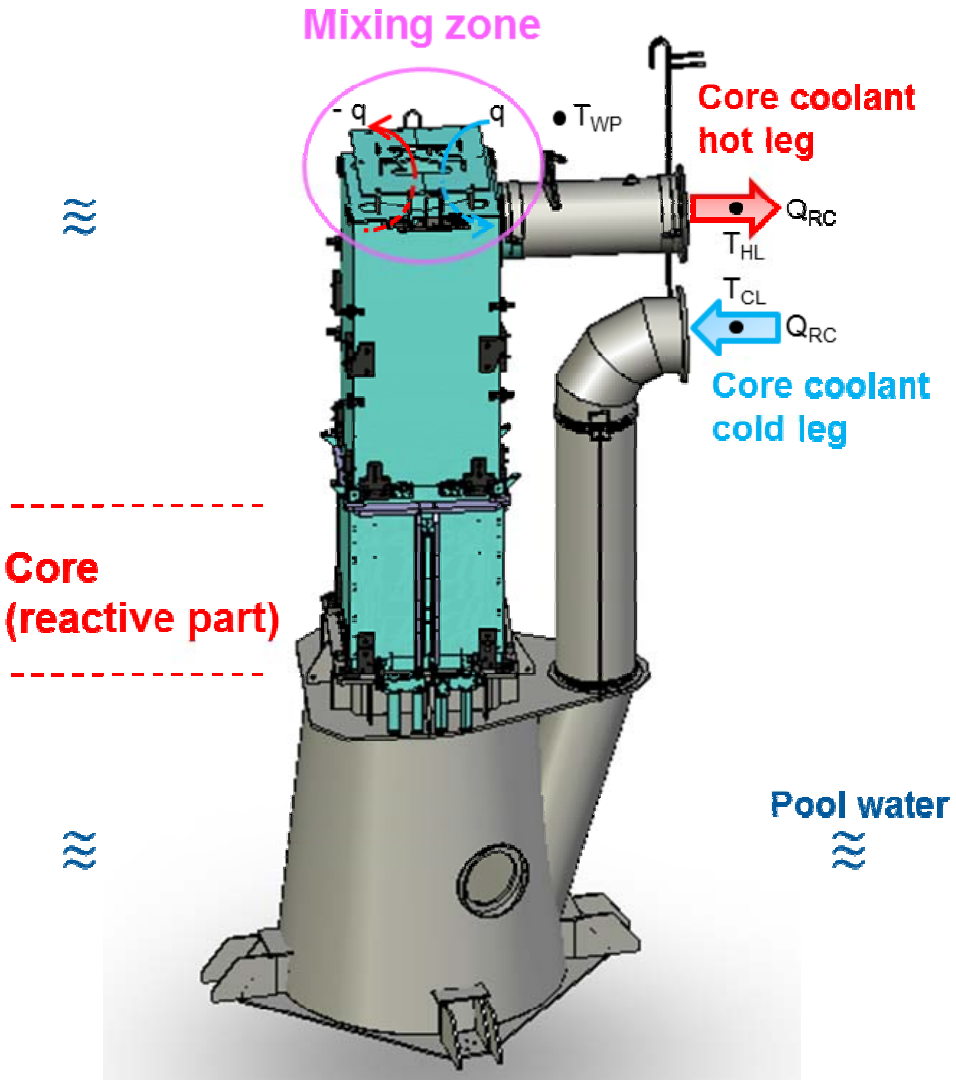

Fig. 4. Mixing zone in the upper water box area (the 6 hafnium control rods and the experimental pressurized water loop are not represented in this figure)

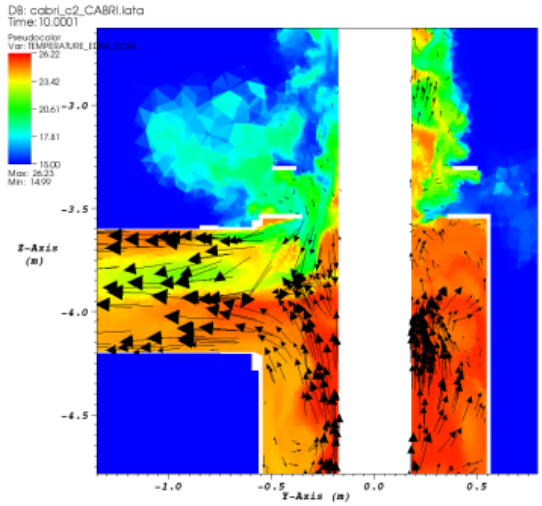

Fig. 5. Mixing zone calculated with the 3D TRIO-U code

The thermal balance used to calibrate the neutron power chambers, is performed on the core water cooling circuit by means of Pt100 probes located downstream of the upper water box. It is therefore necessary to consider this ingress of cold water in the assessment of the core power.

Therefore, an experimental methodology was defined to validate the computations and to reassess the core power taking into account this ingress of pool water.

4.2 Experimental reassessment of the CABRI core power

4.2.1 Calibration of the ionization chambers

The core power is measured by means of boron ionization chambers. During the commissioning tests these neutron detectors will have to be calibrated thanks to thermal balances performed on the core water cooling circuit.

This calibration process is essential as the core power measurement during the power excursions only relies on these neutron detectors.

During a thermal balance, the calibration of the ionization chambers, that is to say the assessment of the neutron detector sensitivity coefficient, c , relies on the following equations:

$$P_{ND} = c.S \quad (1)$$

$$P_{ND} = P_{TB} \quad (2)$$

$$P_{TB} = \rho.C_p.Q_{RC}.\left(T_{HL} - T_{CL}\right) + P_{TL} \quad (3)$$

$$P_{TL} = K.\left(T_{HL} - T_{PW}\right) \quad (4)$$

With

P_{ND} core power measured by the boron ionization chambers (Neutron Detectors) (W)

c neutron detector sensitivity coefficient (W/V), depending on the detector temperature (to be evaluated during thermal balances)

S detector signal (V) (measurement)

P_{TB} core power measured by Thermal Balance (W)

ρ water density (kg/m^3)

C_p water isobar specific heat (J/kg.°C^{-1})

Q_{RC} Reactor Coolant flow rate (m^3/s) (measurement – Q_{RC} ~ 3200 m^3/h = 0.89 m^3/s)
T_{HL} water temperature in the core coolant Hot Leg (see Fig. 4) (°C) (measurement)
T_{CL} water temperature in the core coolant Cold Leg (see Fig. 4) (°C) (measurement)
P_{TL} Thermal Leak through the upper box (see 4.1) (W)
K thermal leak coefficient (W/°C)
T_{PW} Pool Water temperature (°C) (measurement)

The thermal leak coefficient, K, directly proportional to q, was computed to $2.3.10^{+5}$ W/°C (see paragraph 4.1). In order to validate this computation, an experimental methodology was defined. The chapter that follows describes that methodology.

4.2.2 Experimental assessment of the thermal leak coefficient, *K*

The mixing zone always exists as soon as the cooling circuit operates, even outside power operating phases of the reactor. In that case, from above equations (3) and (4) one can write:

$$\rho.C_p.Q_{RC}.(T_{HL}-T_{CL}) = -P_{TL} = -K.(T_{HL}-T_{PW}) \qquad (5)$$

Thus, the thermal leak coefficient K will be determined empirically from experimental data (see Fig. 6). The experimental values corresponding to the left hand side of Fig. 6 will be obtained when the temperature of the pool water will be higher than the temperature of the reactor coolant ($T_{PW} \geq T_{HL}$), for example after a cooling period of the reactor coolant in the storage tank. Whereas the ones corresponding to the right hand side of Fig. 6 will be obtained when the temperature of the pool water will be lower than the temperature of the reactor coolant ($T_{PW} \leq T_{HL}$), for example after an operating phase at limited power (Core power < 15 MW) in order to be sure to meet the maximum core power (25 MW) during the calibration process.

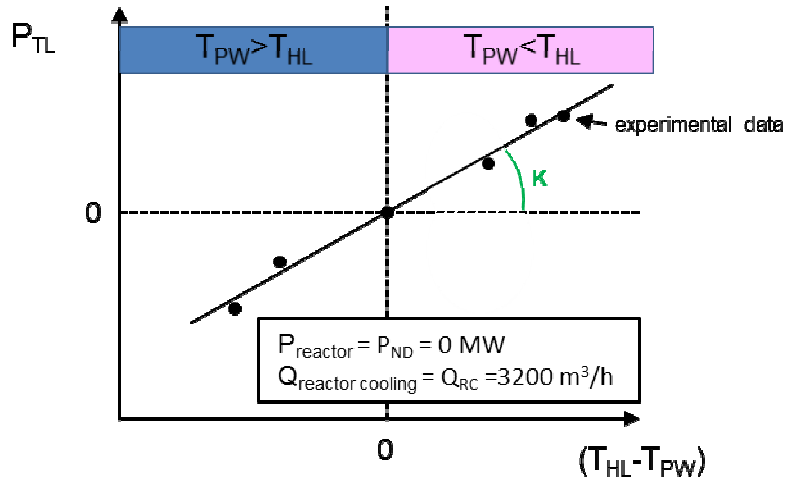

Fig. 6. Thermal leak through the upper water box as a function of $(T_{HL}-T_{PW})$

The experimental assessment of the thermal leak coefficient, K, will allow the validation of the calculations using the 3D TRIO U code (see paragraph 4.1).
Therefore, the calibration of the ionization chambers will be performed with a good accuracy taking into account the ingress of cold water through the upper water box in the thermal balance (see paragraph 4.2.1).

5 Assessment of the injected energy in the experimental fuel rod

5.1 Equations

The injected energy in the experimental fuel rod during the power excursion, together with the power transient width at mid-height, are the two main objectives of the tests conducted on CABRI.

The injected energy in the experimental fuel rod at peak power node, E_{EFR_PPN}, satisfies the following equations:

$$E_{EFR\_PPN} = \frac{E_{core}.FF}{C.M} \qquad (6)$$

$$E_{core} = \int P_{ND}.dt \qquad (7)$$

With:

E_{EFR_PPN}	injected energy in the Experimental Fuel Rod at Peak Power Node (J/g, but usually in cal/g)
E_{core}	core energy (J)
FF	Form Factor (without unit) (measured with the Hodoscope[5] device during a reactor power plateau)
C	coupling factor (measurement, see § 5.2 below)
M	mass of the experimental fissile column (g) (computation performed with METEOR or TOSUREP codes)
P_{ND}	core power measured by the boron ionization chambers during the power excursion (Neutron Detectors) (W) (see § 4.2.1 and [3])

5.2 Coupling factor measurement

The coupling factor C is the ratio between the core power (P_{ND}, measured by the power chambers) and the fissile power generated by the test rod (P_{TR}):

$$C = \frac{P_{ND}}{P_{TR}} \qquad (8)$$

C will be measured before the test, during a reactor power plateau by performing a thermal balance on the water of the experimental loop in the same thermalhydraulic conditions of the test ones (i.e. between 280°C and 300°C and 155 bars).

During this thermal balance performed in steady-state conditions, P_{TR} will satisfy (see Fig. 7):

$$P_{TR} = P_{TC} - P_{\gamma} \qquad (9)$$

$$P_{TC} = \rho.C_p.Q_{TC}.(T_{OC} - T_{IC}) \qquad (10)$$

$$P_{\gamma} = C_{\gamma}.P_{ND} \qquad (11)$$

With:

P_{TR}	fissile power generated by the Test Rod (W)
P_{TC}	thermal power evacuated by the coolant in the Test Channel (W)
P_{γ}	γ-heating of the pressurized water in the test channel (W)
ρ	water density (kg/m^3)
C_p	water isobar specific heat (J/kg.°C^{-1})
Q_{TC}	water flow rate in the Test Channel (m^3/s) (measurement)
T_{OC}	water temperature at the Outlet of the test Channel (°C) (measurement)

[5] Hodoscope : IRSN device; it includes 153 neutron detectors to follow the experimental rod fuel motion during the test.

T_{IC} water temperature at the Inlet of the test Channel (°C) (measurement)

C_{γ} γ-heating coefficient (W/ MW of core power) (computed to 67 W for 1 MW of reactor power, will be evaluated during the commissioning tests)

P_{ND} core power measured by the boron ionization chambers (Neutron Detectors) (W in equation (8), MW in equation (11)) (measurement) (see § 4.2.1)

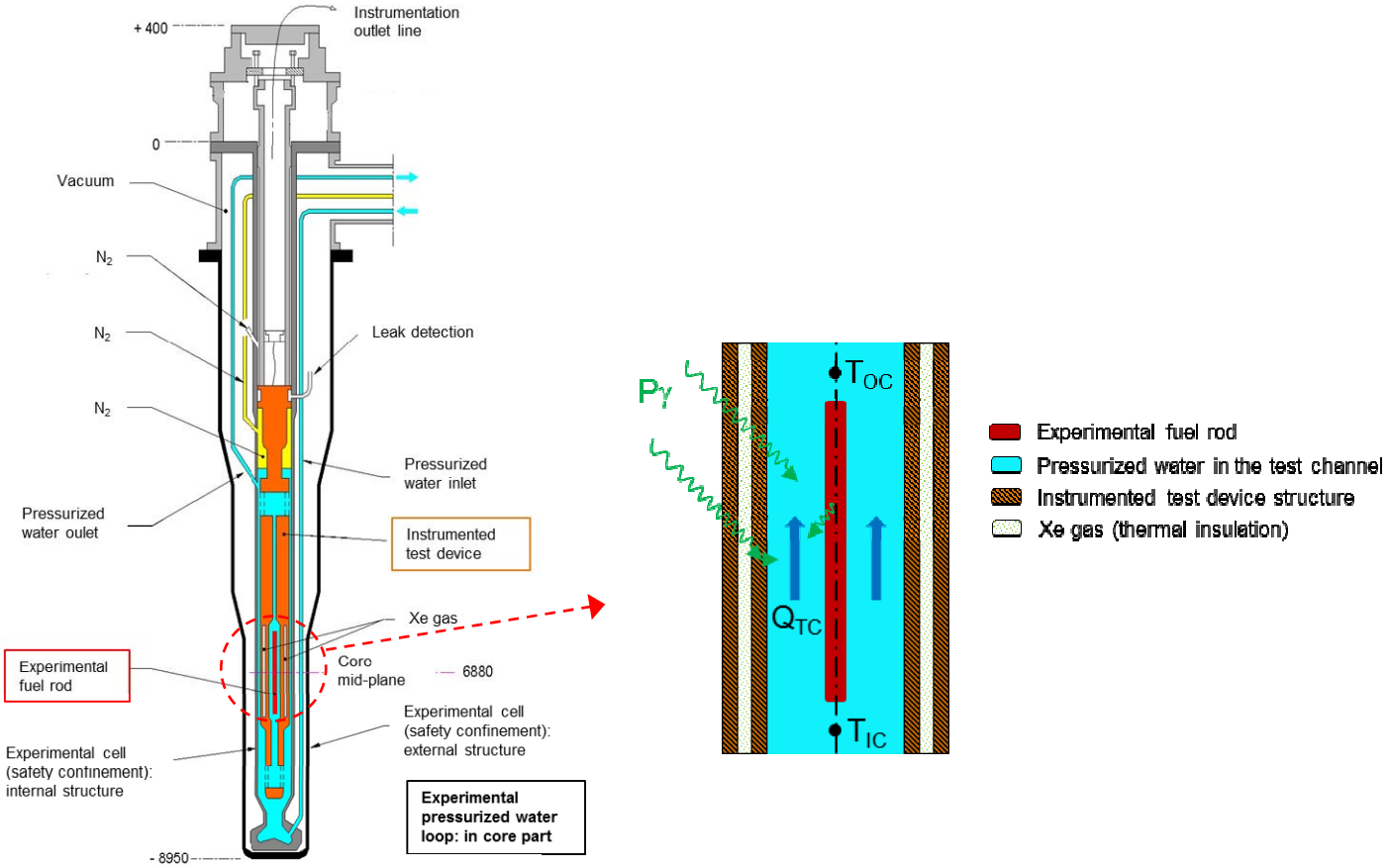

Fig. 7. Coupling factor measurement

Thus, the experimental assessment of the coupling factor during a reactor power plateau will allow the assessment of the injected energy in the experimental fuel rod during the power excursion.

6 Measurement uncertainties

6.1 General presentation

In order to access to the assessment of the final uncertainty on the injected energy (which is the objective of the experimental protocol), we followed the methodology elaborated by the *Bureau International des Poids et Mesures* [6]. Documents have been published [7], [8], [9], [10]. The document [8] is a true guide for people in charge of experiments in their works generating measurements. We have followed their recommendations. First we begin by describing the physical variable we wish to measure and the measurement process used. The latter generally contains imperfections which cause an error in the measurement result. Then the work consists in identifying as well as possible the causes of measurement errors in order to evaluate in the best way possible the corrections entailed by these errors. The

corrections (or systematic errors) applied to the rough observations are mainly corrections linked to the calibration or to the integration of the experimental conditions. The detection of the former requires an actual audit of the people directly involved in the instrumentation. The detection of the second (integration of the experimental conditions) is the consequence of a general view of the experiment obtained through the analysis of coherence of the announced results. The corrections are applied to get as close to the real value of the physical variable. The uncertainties on the rough values and the corrections applied are then evaluated through methods of type A if we are in the presence of several measurements (statistic evaluation) or of type B (use of extra knowledge, constructor documentations for instance) if there is only one measurement. In the case where the physical variable Y is not directly measurable but is obtained using the values of a set of other orders of magnitude, we will attempt to model the measurement process of Y in the following way:

$$Y = f(X_1, X_2, ..., X_n)$$

in which the X_i represent the entry values necessary to calculate Y through the explicit function f. The X_i values can represent:

- results on rough measurements
- calibration corrections
- corrections of experimental environments
- any other parameter deemed necessary in correctly evaluating the value Y

The uncertainty on Y is called ***composed uncertainty***, this is to insist on the fact that it is calculated by taking into account all the sources of influence. It is noted u_c. And we use the law of propagation of uncertainty (12) to calculate it:

$$u_c^2(y) = \sum_{i=1}^{n}\left[\frac{\partial f}{\partial X_i}\right]^2 u^2(x_i) + 2\sum_{i=1}^{n-1}\sum_{j=i+1}^{n}\frac{\partial f}{\partial X_i}\frac{\partial f}{\partial X_j}u(x_i, x_j) \quad (12)$$

Fig. 8 presents all the measurements which have been qualified. We can thus place them with convenience in the overall Energy assessment.

6.2 Uncertainty on the CABRI core power

We correct the systematic error on the thermal balance core power highlighted by the simulation study presented in section 4. We then propagate the uncertainties through the application of the law of propagation of uncertainty (eq. 12).

6.2.1 Uncertainty on the Thermal Balance core Power P_{TB}

Concerning the Thermal Balance core Power P_{TB} the principal step, presented in the section 4, is to take into account the leak which was highlighted into the water of the pool. We will have to assess the Thermal Leak Power P_{TL} (cf. section 4.2.2, Fig. 6) doing a simple linear regression fitting the model:

$$P_{TL} = K.(T_{HL} - T_{PW}) + \varepsilon$$

where K is the slope and ε follows a normal distribution with constant variance σ^2 and zero mean. Then, the uncertainty on an individual thermal leak power value is given by the uncertainty on a predicted value that is to say:

$$u^2(P_{TL}) = \sqrt{(T_{HL} - T_{PW})^2.u^2(K) + \sigma^2}$$ ($u(K)$: standard deviation on the slope)

Once the P_{TL} is evaluated, we will apply the correction for the P_{TB} calculation:

$$P_{TB} = P_{rawTB} + P_{TL} = \rho.C_p.Q_{RC}.(T_{HL} - T_{CL}) + P_{TL}$$

and we propagate the uncertainties (***step 1*** on Fig. 8):

$$u_c^2(P_{TB}) = u_c^2(P_{rawTB}) + u_c^2(P_{TL})$$ since P_{TB} and P_{TL} are not correlated

This calculation represents in fact the uncertainty on the standards that will be used in the next section to estimate the calibration surface for the P_{ND} assessment. Fig. 9 (a), obtained

from simulated data, shows that the uncertainty increases proportionally to the thermal balance power. Thus, in the framework of the CABRI experiments, that is to say from 8 MW to 25 MW (commissioning phase), relative uncertainty varies from 4% to 2%. We will have to take into account this characteristic. The numerical application of the law of propagation of uncertainty indicates that the uncertainty on P_{TL} can play a major rule in the global variance on P_{TB} .

Hence, during the commissioning phase, it will be very important to set up the experimental conditions to assess the temperature discrepancy $\Delta T = T_{HL} - T_{PW}$ with the best precision in order to reduce the uncertainty on P_{TL} through the linear regression.

6.2.2 Uncertainty on the boron ionization chambers calibration

Once the P_{TB} standards estimated with their uncertainties, the calibration of the ionization chambers is performed taking into account the relationship between these values and the boron ionization chambers signal. The calibration model depends on the physics of the neutron detection phenomenon. The detector response is sensitive to the temperature of the pool water near the detector. In the past, we used to do the calibration in two steps. First, we did the calculation of the ratio:

$$c = \frac{P_{TB}}{S}$$

then a linear regression between c and the temperature T_{ND}:

$$c = a - b.T_{ND}$$

We have decided now to realize the regression in one step using a non linear model (***step 2*** on Fig. 8):

$$S = \frac{b_1.P_{TB}}{\left(1 + b_2.T_{ND}\right)}$$

Fig. 9 (b) shows the shape of this calibration surface and highlights the CABRI field ($0° \le T \le 45°C - 0 \le P \le 25MW$).

From the old Na experiments we use a number of 12 samples of thermal balance core power to establish the relationship between a measured boron ionization chamber signal and the thermal balance power. During the test, this relationship is then used to estimate the unknown power from the boron ionization chamber signal inverting the formula :

$$P_{ND} = \frac{S.\left(1 + b_2.T_{ND}\right)}{b_1} \quad \textit{inverse calibration} \ (13)$$

In addition to the estimates themselves, we search for having available some measure of their precisions, usually given in the form of confidence limits. The values of b1, b2 are reached by the use of a classical non linear method. In our case, we also have to introduce the influence of the following constraints:

- The P_{TB} uncertainty (the P_{TB} values correspond to the standards)
- The S uncertainty (Neutrons Detector)
- The T_{ND} uncertainty (Temperature of the Detector)
- The small size of the experimental sample

We decide to process as the following :

1. Firstly we realise the non linear regression with the initial data set.
2. Then we generate artificially 999 other samples, called replica using the bootstrap methodology [11] (step 4 below). For every new sample we calculate the non linear regression.
3. During the generation of every bootstrap sample (i.e. for every replica), we replace every value of standards by a random value obtained from a Gaussian distribution with mean equal to the measurement value and standard deviation given by the

regression presented in Fig. 9 (a). The values of the ionization chambers are replaced by random values extracted from a normal law with mean the average of the signal and relative standard deviation equal to *0.4 %* (Type A estimation from the boron ionization chambers signal).

4. We so obtain a noisy set of the values P_{TB} and S. At this step, we extract a replica from it containing 12 couples (P_{TB}, S) by bootstrap which consists to create new samples of equal size from the measured dataset, each of which is obtained by random sampling with replacement from the original dataset. On every replica, we make a non linear regression. This process is repeated 999 times which gives with the initial regression 1000 pairs (b_1, b_2) so 1000 results of non linear regression.
5. For values of P_{TB} fixed we calculate the predicted S value by using the result of the initial non linear regression. In the experimental phase this value is given by the boron ionization chambers.
6. Then we generate a set of values around this value according to a Gaussian law of mean the predicted value with a relative standard deviation equal to *0.4%* (a size of 100 for example).
7. For each of these 100 S values we calculate for every bootstrap pair result (b1,b2) the inverse values in P_{ND} using equation (13), fixing the value of temperature T_{ND}. We so obtain 100 x 1000 inverse values for P_{ND}.
8. Then using these 100 x 1000 values we calculate the mean to estimate the inverse value in power and the quantiles at *2.5 %* and *97.5 %* levels to obtain the *95%* reliable interval around this inverse value.

In the step 7 above, the inverse values P_{ND} calculated for each 100 S values are obtained through every model (b_1, b_2) represented by a red point on the Fig.10 (a). All the inverse predictions give thus the possibility to assess the quantiles for a P_{ND} value.

We can have an idea of the P_{ND} repartition on the Fig.10 (b) for some joint values of core power and temperature.

According to these results, we *can thus assess*
a relative uncertainty around 4 % on P_{ND} *in the field of CABRI conditions.*

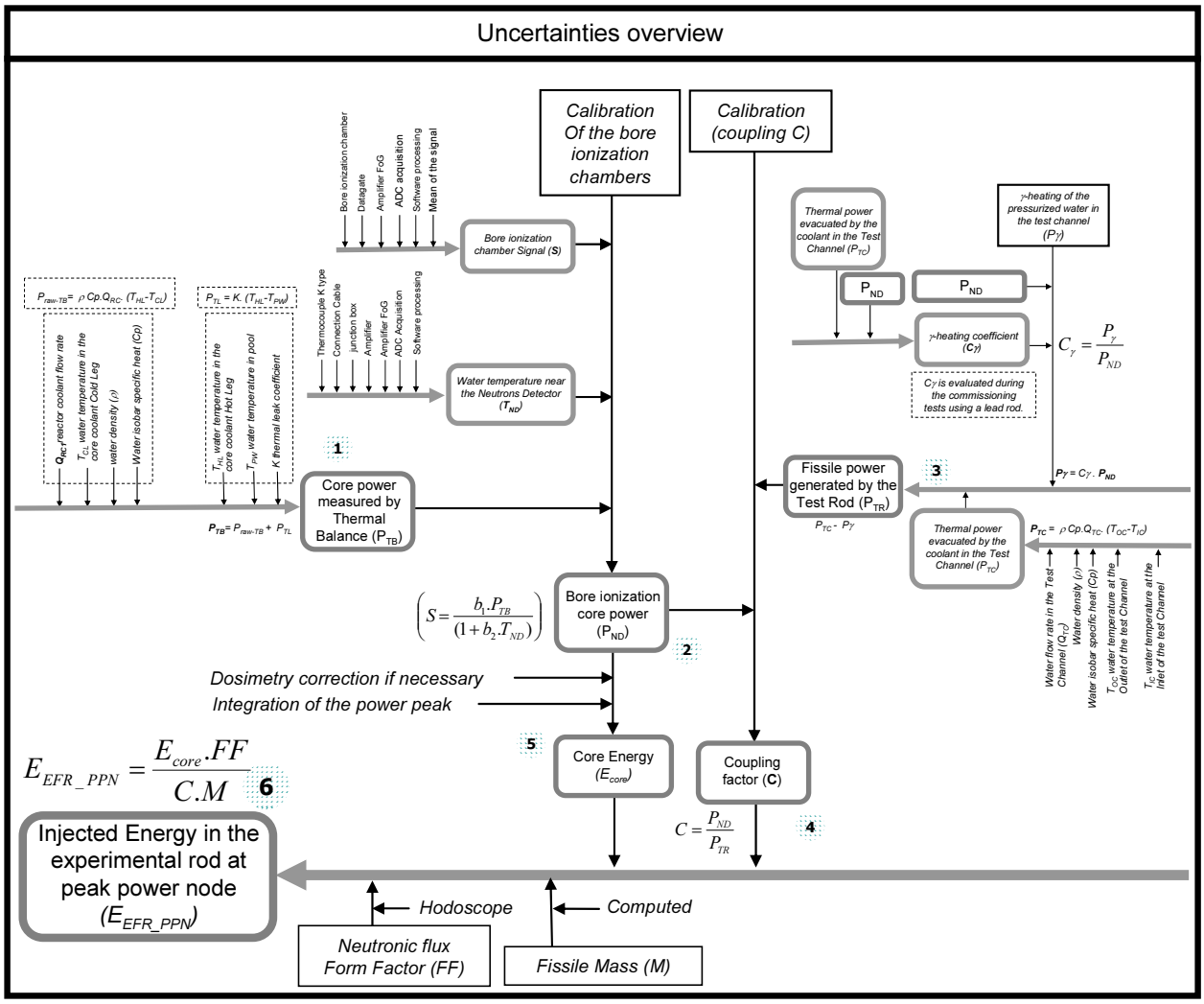

Fig. 8. Uncertainties overview

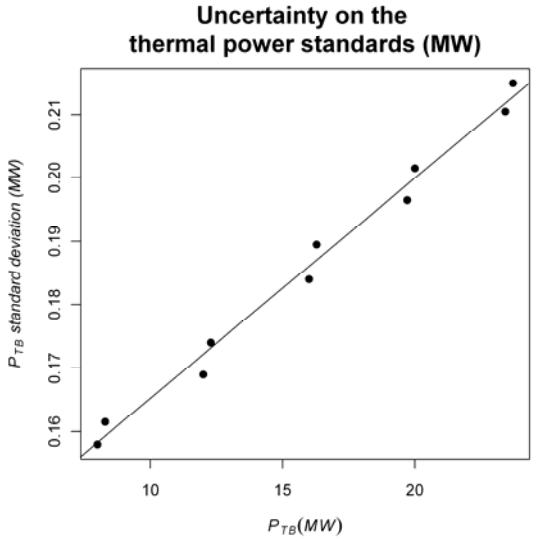

(a) Uncertainties on the thermal balance core power standards are not constant according to the order of magnitude

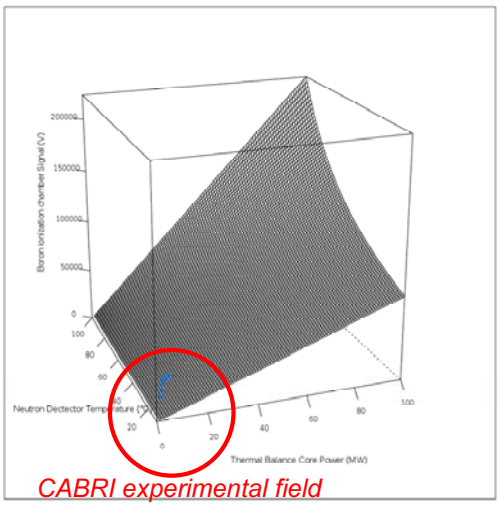

(b) Visualization of the Calibration surface of the boron ionization chambers

$$S = \frac{b_1.P_{TB}}{(1+b_2.T_{ND})}$$

Fig. 9. The uncertainty of the P_{TB} has to be taken into account for the non linear regression

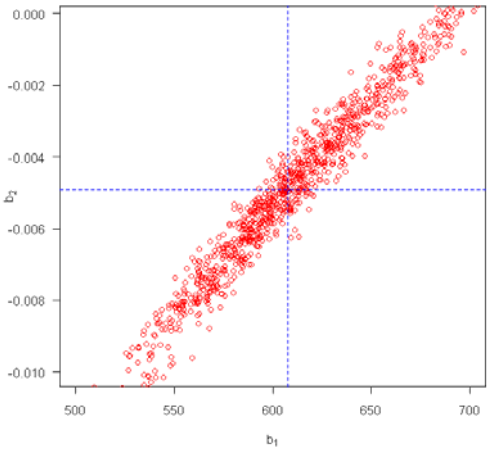

(a) Visualization of the 1000 non linear regression results (b_1,b_2)

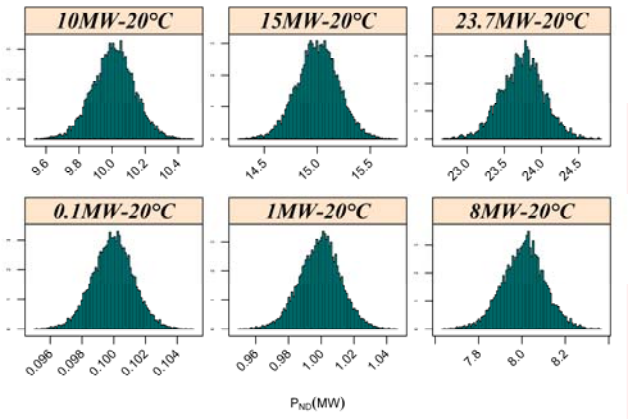

(b) Repartition of the inverse P_{ND} values for some artificial joint values of core power and temperature

Fig. 10. Percentiles assessments for an inverse P_{ND} value

6.3 Uncertainty on the injected energy in the test rod

6.3.1 Uncertainty on P_{TR} during the thermal balance

We have the relation: $P_{TR} = P_{TC} - P_{\gamma}$ with $P_{\gamma} = C_{\gamma}.P_{ND}$. (see section 5.2).

The C_{γ} coefficient will be estimated during the commissioning phase (***step 3*** on Fig. 8).

We deduce its uncertainty: $u_c^2(P_{TR}) = u_c^2(P_{TC}) + u_c^2(P_{\gamma})$ with $u_c^2(P_{\gamma}) = P_{ND}^2.u_c^2(C_{\gamma}) + C_{\gamma}^2.u_c^2(P_{ND})$

6.3.2 Uncertainty on the coupling factor C during the thermal balance

The C coefficient corresponds to the ratio:

$$C = \frac{P_{core}}{P_{TR}} = \frac{P_{ND}}{P_{TR}}$$ (see section 5.2 and ***step 4*** on Fig. 8).

Hence: $u_c^2(C) = \left(\frac{1}{P_{TR}}\right)^2 u_c^2(P_{ND}) + \left(\frac{-P_{ND}}{P_{TR}^2}\right)^2 u_c^2(P_{TR})$

We assume that the factor coupling is constant during the transient, that is to say it doesn't depend on the core power.

6.3.3 Uncertainty on E_{core} during the experimental phase

The time integration of the power measured by P_{ND} during the transient provides us with the energy. Thus, the uncertainty is the same that the P_{ND} uncertainty. Possibly, the signal will be corrected according to the values of dosimeters which will be placed into the CABRI reactor (***step 5*** on Fig. 8).

6.3.4 Uncertainty on the injected energy during the experimental phase

The injected energy is given by the equation (see section 5.1):

$$E_{EFR\_PPN} = \frac{E_{core}.FF}{C.M}$$ (***step 6*** on Fig. 8)

All physical variables are independent except perhaps the coupling factor with the core

Energy. We already mentioned in the § 6.3.2 that the factor coupling is supposed constant during the transient, that is to say it doesn't depend on the core energy. Thus the correlation between E_{core} and C is equal to zero in the formula (12).

We obtain:

$$u_c^2\left(E_{EFR\_PPN}\right)=\left(\frac{FF}{C.M}\right)^2 u_c^2\left(E_{core}\right)+\left(\frac{E_{core}}{C.M}\right)^2 u_c^2\left(FF\right)+\left(\frac{-E_{core}.\frac{FF}{M}}{C^2}\right)^2 u_c^2\left(C\right)+\left(\frac{-E_{core}.\frac{FF}{C}}{M^2}\right)^2 u_c^2\left(M\right)$$

Finally, doing the numerical application from the precedent equation, we obtained an uncertainty of 11% on the injected energy

7 Conclusion

This study presents the experimental method defined to assess the power of the CABRI core, and thus, the injected energy in the experimental fuel rod. In particular, this method takes into account the ingress of pool water into the newly designed upper water box during thermal balances performed on the core water cooling circuit (calibration phase of the neutron power chambers).

The application of the uncertainty analysis process shows that the measurement of this Thermal Leak Power could be an important parameter in the global variability. We will have to assign a high – level of importance to the measurements of the temperature in order to very well assess the temperature discrepancy. The systematic errors assigned to every Pt100 temperature probe will be done during the isothermal phase.

According to data from old Na tests, we are able to propose a new method to assess the uncertainty related to the core power deduced from the ionization boron chamber signal taking into account the uncertainties on the standards (Thermal Balance core Power P_{TB}), the boron ionization chambers signal (S) and the temperature of the Neutrons Detectors (T_{ND}). We obtained an uncertainty around *4 %*. This new method will be applied during the commissioning phase in order to adjust this value with the new facility. In order to improve the adjustment, it will be worth to do experimental points in temperatures of functioning covering the whole experimental field.

After evaluating the core power from the ionization boron chamber signal, the delta method propagates the uncertainties to access the final uncertainty on the injected energy leading finally to a global relative uncertainty around *11%*.

8 REFERENCES

[1] J. Estrade, G. Ritter, D. Bestion, J.C. Brachet, Y. Guérin, O. Guéton, Upscaling CABRI core knowledge for a new safety case, RRFM 2009, Vienna, Austria.

[2] G. Ritter, F. Rodiac, D. Beretz, C. Jammes, O. Guéton
Neutron commissioning in the new CABRI water loop facility, IGORR 2010, Knoxville, TN, USA.

[3] G. Ritter, F. Rodiac, D. Beretz, J.M. Girard, O. Guéton
Core characterization of the new CABRI water loop facility, ISRD 2011, Bretton woods, NH, USA.

[4] G. Ritter, J. Fache, L. Pantera
An ideal tool for criticality level prediction, RRFM 2011, Roma, Italy

[5] G. Ritter, R. Berre, L. Pantera, F. Jeury
DULCINEE. Beyond neutron kinetics, a powerful analysis software, RRFM IGORR 2012, Prague, Czech Republic

[6] BIPM (Bureau International des Poids et Mesures)
http://www.bipm.org/en/publications/guides/gum.html

[7] Evaluation of measurement data – Guide to the expression of uncertainty in measurement JCGM 104:2009

[8] Evaluation of measurement data – An introduction to the "Guide to the expression of uncertainty in measurement and related documents" JCGM 104:2009

[9] Evaluation of measurement data – Supplement 1 to the "Guide to the expression of uncertainty in measurement and related documents" - Propagation of distribution using a Monte Carlo method JCGM 101:2008

[10] Christophe Bindi
Dictionnaire pratique de la métrologie, Mesure, essai et calculs d'incertitudes AFNOR 2006

[11] A.C. Davison and Diego Kuonen An Introduction to the Bootstrap with Applications in R
Statistical Computing & Statistical Graphics Newsletter Vol.13 No1